

Synthesis and zinc(II) complexation modulated fluorescence emission properties of two pyrene-oligo(phenylene vinylene)-2,2'-bipyridine conjugated molecular rods†

Stéphanie Leroy-Lhez,^{*a} Magali Allain,^a Jean Oberlé^b and Frédéric Fages^{*c}

Received (in Durham, UK) 30th November 2006, Accepted 21st March 2007

First published as an Advance Article on the web 19th April 2007

DOI: 10.1039/b617497c

A series of conjugated rods in which the pyrene chromophore is connected to a 2,2'-bipyridine unit *via* an oligo(phenylene vinylene) bridge have been synthesized and their photophysical properties in solution investigated. They are shown to display intense visible electronic absorption and fluorescence emission properties. The excited-states characteristics are compared to analogous systems containing an oligo(phenylene ethynylene) spacer. The zinc complexes of the new molecules possess very polar excited states, which lead to strong solvatochromic shifts. Semi empirical calculations were performed which confirmed the experimental data. The X-ray analysis of a pyrene-containing π -conjugated bipyridine ligand is described.

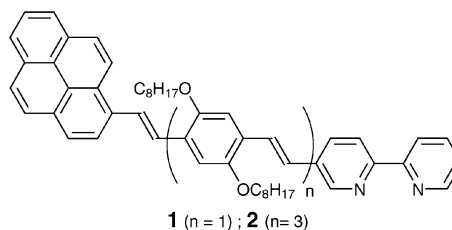
Introduction

Molecular rods represent a fascinating class of molecules that are the subject of a tremendous interest because of their applications in many areas.^{1,2} Among this broad class of systems, oligo(phenylene vinylene) (OPV)-based materials have received considerable attention. They have been employed as active layer in organic light-emitting diodes,³ organic field effect transistors,⁴ and in solar cells,^{5,6} liquid crystals,⁷ or as building blocks in dendrimers,⁸ functional nanostructures^{9,10} and hybrid materials.¹¹ OPVs have been long known to have versatile light-emission properties both in solution and the solid state.¹² As such they represent attractive scaffolds on which to base the design of molecular systems and materials with stimulative fluorescence emission characteristics.^{13–17}

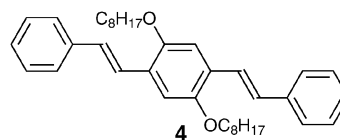
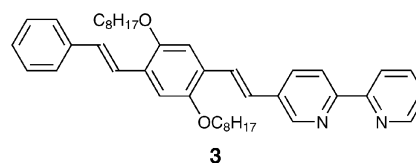
In that connection, the incorporation of the 2,2'-bipyridine unit into conjugated backbones has led to highly fluorescent chromophores with interesting metal ion sensory properties.¹⁸ For example, 2,2'-bipyridine-containing poly(phenylene vinylene) were reported as luminescent materials exhibiting highly ionochromic effects as a result of the interplay between photophysical and complexation properties.^{19–21}

Recently,²² we showed that a properly designed conjugated molecular rod, **1**, in which the pyrene chromophore and the 2,2'-bipyridine ligand unit are connected *via* an OPV bridge could give rise to spectacular changes in optical responses depending on the nature of the solvent and the presence of

metal ions. A series of analogous systems based instead on the oligo(phenylene ethynylene) (OPE) backbone in which the subunits are connected through acetylenic linkages were investigated and also displayed remarkable tunable fluorescence and luminescence emission properties.^{23–25}



In this paper, we present the synthesis and a photophysical study of compound **1** and a series of related compounds. Especially, information on the influence of conjugation enhancement and terminal aromatic group on the excited state properties are provided by compounds **2** and **3**, respectively. The results outline the occurrence of a polar singlet excited state in the free ligands and their corresponding zinc(II) complexes, which gives rise to highly solvatochromic shifts of the fluorescence emission maximum. The experimental results are strongly supported by theoretical calculations and are discussed in the light of the data obtained for related OPE-based molecular rods.

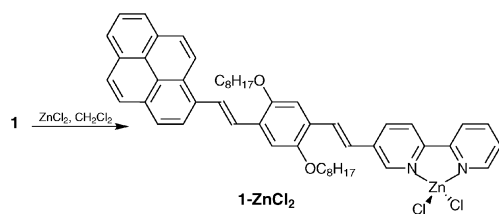


^a CIMMA UMR 6200 CNRS, Université d'Angers, UFR Sciences, 2 Bd Lavoisier, 49045 Angers Cedex, France. E-mail: stephanie.lhez@univ-angers.fr

^b CPMOH UMR 5798 CNRS, Université Bordeaux 1, 352 Cours de la Libération, 33405 Talence Cedex, France

^c GCOM2 UMR 6114 CNRS, Université de la Méditerranée, Faculté des Sciences de Luminy, Case 901, 13288 Marseille Cedex 9, France. E-mail: fages@luminy.univ-mrs.fr

† CCDC reference numbers 641181. For crystallographic data in CIF or other electronic format see DOI: 10.1039/b617497c



Scheme 1 Synthesis of zinc(II) complex **1-ZnCl₂**.

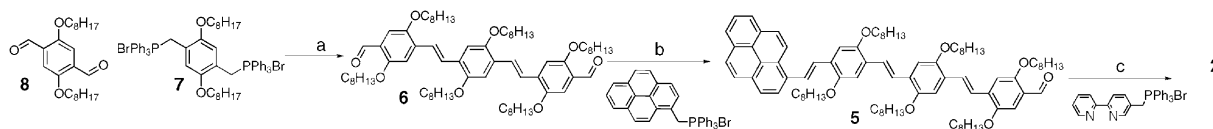
Results and discussion

Synthesis

The syntheses of ligands **1–3** and reference compound **4** are based upon classical Wittig-type olefin bond formation methodology followed by iodine-catalysed isomerization. The all-*trans* configuration was assessed by ¹H NMR spectroscopy for all compounds and confirmed by X-ray crystallography analysis in the case of **1**.

The synthesis of both pyrene-2,2'-bipyridine compounds **1** and **3**, containing one phenylene-vinylene unit as a spacer, followed a one-pot procedure involving two Wittig reactions between the bis-phosphonium salt derivative of 1,4-bis(bromomethyl)-2,5-bis(octyloxy)benzene, **7**,¹⁹ and a mixture of 2,2'-bipyridine-5-carbaldehyde²⁶ and benzaldehyde or pyrene-1-carbaldehyde. This statistical method afforded inevitably a mixture of symmetrical and dissymmetrical oligomers, but all of them could be easily separated by column chromatography owing to their markedly different polarity. Reference compound **4** was also obtained by reacting **7** and benzaldehyde in a 1 : 2 molar ratio. Oligomers **3** (11% yield) and **4** (55% yield) were prepared using dichloromethane as solvent and EtOLi as a base, while **1** was obtained (20% yield) in THF in the presence of NaH. The mononuclear zinc(II) complex of **1**, **1-Zn** was obtained by mixing the free ligand and ZnCl₂ in dichloromethane (Scheme 1).²⁷ The purity and the 1 : 1 metal/ligand stoichiometry were confirmed by elemental analysis.

In the case of longest oligomer **2**, containing three phenylene-vinylene units, a stepwise synthetic route was chosen (Scheme 2). It is based on the use of the dialdehyde **6** which was obtained according to published procedure¹⁰ from dialdehyde **8** and the bis-phosphonium salt **7**. Dialdehyde **6** was subjected to a first Wittig reaction using the phosphonium salts of 1-bromomethylpyrene to produce the pyrene-containing mono-aldehyde **5**. The latter was then reacted with the phosphonium salt of 5-bromomethyl-2,2'-bipyridine under the same Wittig conditions to afford the target oligomer **2**. Subsequent iodine-catalysed isomerization afforded **2** in 25% yield from **6** (Scheme 2). Owing to the presence of the alkyl chains on the phenyl rings, all compounds are soluble in common organic solvents.



Scheme 2 Synthesis of compound **2**. Reagents and conditions: (a) EtOLi, CH₂Cl₂, rt, 81%; (b) EtOLi, CH₂Cl₂, rt, 52%; (c) EtOLi, CH₂Cl₂, rt then I₂, CH₂Cl₂, rt, 47%.

The ¹H NMR spectra of free ligands were recorded at room temperature in CDCl₃ or CD₂Cl₂ as solvent (*ca.* 15 mM) (Fig. 1). The assignment of the proton resonances was performed by comparison of the spectra obtained for **1**, **2**, **3** and **4** and using literature data.^{27,28} In the case of compound **1**, a COSY experiment (Fig. 2) allowed full confirmation of the assignment. Typical coupling constant values for *trans*-ethylenic configuration (*ca.* 16–17 Hz) were found.

Single orange crystals of compound **1** were obtained by slow evaporation of a mixture of dichloromethane–methanol and analyzed by X-ray diffraction (Fig. 3). The 2,2'-bipyridine unit is in *trans* conformation with a small torsion angle of 14.4(1)^o between the two pyridine rings. The dihedral angles between the two planes formed by pyrene or bipyridine and the central benzene ring are respectively 175.4(1)^o and 36.5(1)^o.

Photophysical properties of the free ligands

Electronic absorption. Electronic absorption spectra of compounds **1–4** were recorded in toluene and THF at room temperature. They are given in Fig. 4 and the photophysical data are collected in Table 1. All compounds show a broad and intense low-energy absorption band in the visible region except **4** which absorbs in the near-UV. For all pyrene-containing compounds, the spectra are characterized by a single absorption band, whereas for **3** and **4** two bands are clearly observed. In those compounds, the high-energy band is likely to arise from the small axis-polarized transition. When the oligomer length increases, such as in **1** and **2**, the intensity of this band is known to decrease and the lowest-energy transition, which is polarized along the long axis, becomes predominant.²⁹ The molar absorption coefficient of the lowest-energy transition band is found to be 45 600 M⁻¹ cm⁻¹ for **1** in THF. This value is much higher than for pyrene and its alkyl-substituted derivatives that are known to possess a forbidden ¹L_b state as lowest-energy excited state.³⁰ In the case of **1**, the long-axis polarized ¹L_a transition is substantially stabilized at the expense of the ¹L_b one as a result of π-conjugation. This effect is even more pronounced in the case of **2** which possesses a molar absorption coefficient of about 111 500 M⁻¹ cm⁻¹ for the lowest-energy transition band in THF.

The bathochromic shift observed when going from **1** to **2** is consistent with the increase of conjugation with oligomer length.^{31–33} Also consistent with an increase of electronic delocalization is the red-shifted absorption of the pyrene-terminated ligand **1** relative to its benzene-containing reference compound **4**. These features are in keeping with those previously reported for OPE-bridged oligomers.²⁴ The fact that the vinylene compounds **1–4** absorb at lower energy (*ca.* +15–30 nm) with respect to the ethynylene systems²⁴ is indicative of a somewhat better conjugation, consistent with previous observations.^{34,35} Moreover, the electronic

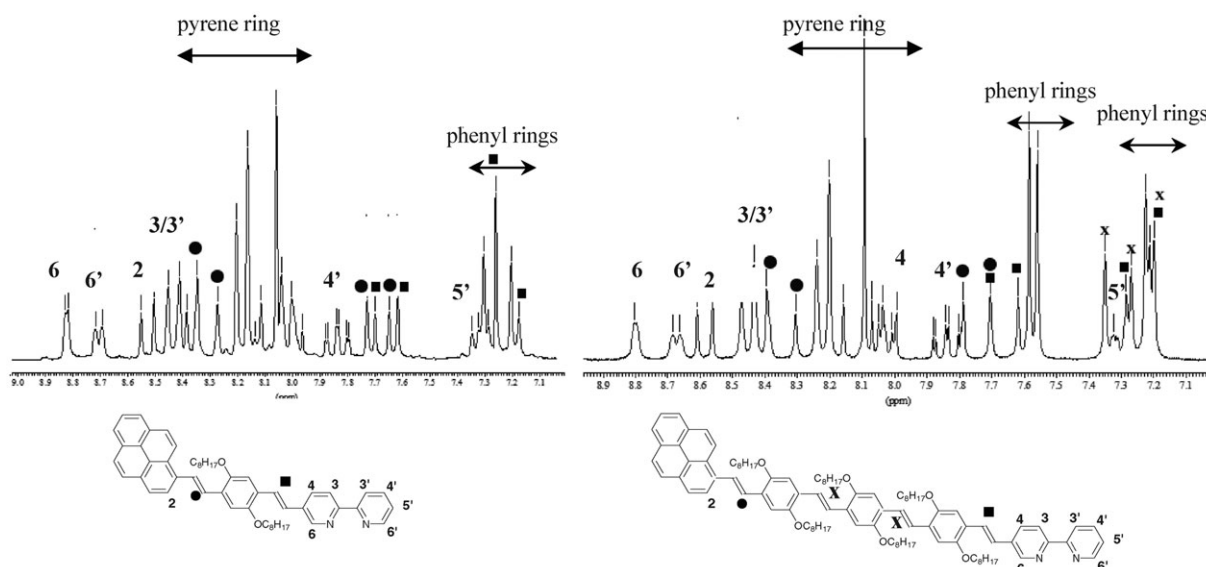


Fig. 1 Aromatic part of the ^1H NMR spectra of ligands **1** (250 MHz, CDCl_3 , 298 K) and **2** (200 MHz, CD_2Cl_2 , 298 K) including the assignment of the protons of the ethylenic bonds between pyrene and phenyl rings (●), between phenyl and bipyridine rings (■), and between phenyl rings (X).

absorption spectra of compounds **1–4** were found to be independent of solvent polarity, which is indicative of the absence of significant charge transfer effect in the ground state, in agreement with previous observations on related pyrene-containing ligands.^{24,30}

Fluorescence emission. Corrected fluorescence emission spectra were recorded in toluene and THF and were found to be independent of the excitation wavelength (Fig. 5). Fluorescence excitation spectra matched the absorption profile over the entire wavelength range.

All compounds are found to be strongly emissive (room temperature fluorescence quantum yields are between 0.5 and 0.8) in the visible range. The progression in the fluorescence maxima from **1** to **4** is found identical to that recorded for the corresponding absorption spectra. It is also noteworthy that fluorescence emission spectra are red-shifted relative to those of OPE-bridged pyrene-bipyridine derivatives,²⁴ which is consistent with the electronic absorption results. The fact that the fluorescence spectra of **1**, **2** and **4** display a clear vibrational structure is also in keeping with the behavior of the acetylenic compounds. The vibronic spacings are found to be *ca.* 1250 cm^{-1} which is in agreement with the stretching modes of aromatic nucleus. In the case of ligand **3**, the vibrational structure was observed only in less polar solvents such as *n*-hexane. The vibronic spacing is then found to be the same as that of the other compounds. The Stokes' shift values in both toluene and THF are in the $2800\text{--}3100\text{ cm}^{-1}$ range, except

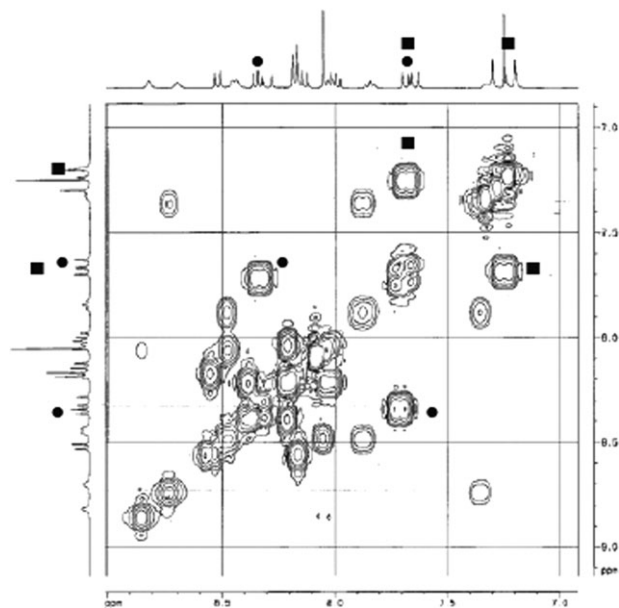


Fig. 2 Part of the 400 MHz COSY $^1\text{H}/^1\text{H}$ spectrum of compound **1** (CDCl_3 , rt) showing the correlations of ethylenic protons between pyrene and phenyl rings (●), and between phenyl and bipyridine rings (■).

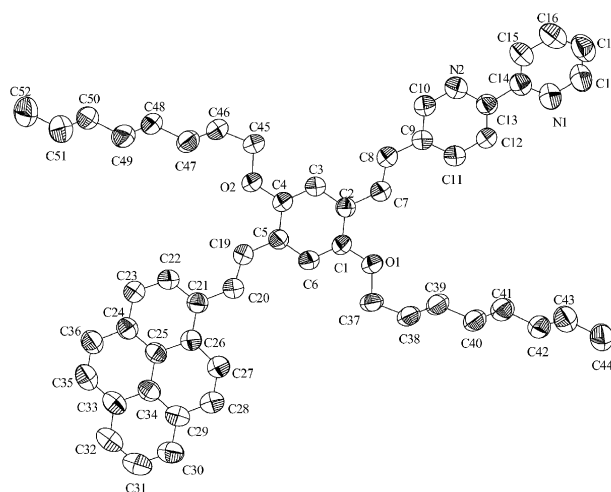


Fig. 3 ORTEP view of crystallographic structure of **1** with 50% probability ellipsoids.

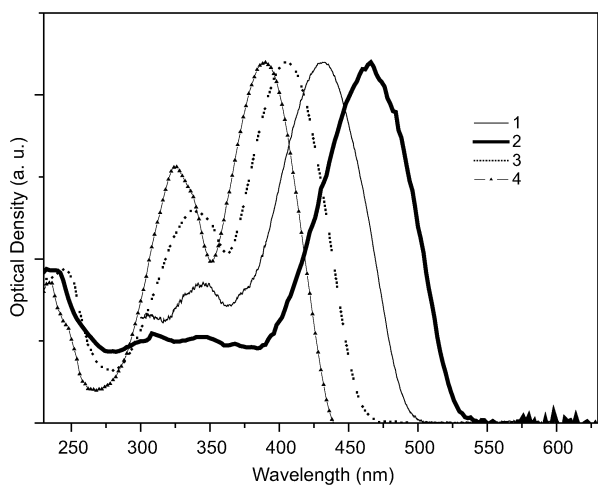


Fig. 4 Normalized electronic absorption spectra of compounds **1–4** in THF (25 °C, $1-5 \times 10^{-6}$ M).

again for **3** for which it depends on the solvent polarity and is hence greater in THF (*ca.* 3500 cm^{-1}). Clearly, these values are between those obtained for bipyridine-pyrene dyads connected by a phenylene-ethynylene bridge²⁴ and those connected by a single C–C bond.³⁰ Moreover, the shape and position of fluorescence spectra were not affected by solvent polarity, which points to the absence of any significant charge transfer character of the excited state in the free ligands.²⁴ Only in the case of **3**, a weak solvatochromic shift was observed.

The fluorescence lifetimes in THF are monoexponential in the nanosecond regime. Ligand **2** displays a particularly short fluorescence lifetime (0.61 ns in THF) compared to the other compounds **1**, **3** and **4**. The radiative rate constants, k_f , and their reduced values, $k_f/n^3\nu^3$,³⁰ were calculated in THF (Table 1). Both values are close to that found for OPE-bridged compounds.²⁴ All together, the photophysical data obtained for **1** and **2** are consistent with the occurrence of a highly allowed $\pi\pi^*$ singlet excited state in which the excited state of the pyrene chromophore exhibits a strong 1L_a character. Such stabilization of the long-axis polarized transition seems to be more effective for vinylic spacers than for acetylenic ones.

Finally, it has to be mentioned that no phosphorescence emission from the ligands could be detected in low temperature THF matrix (77 K) containing 10% of iodobutane. This is not surprising according to the particularly high radiative decay rate constants obtained for these compounds.^{24,36}

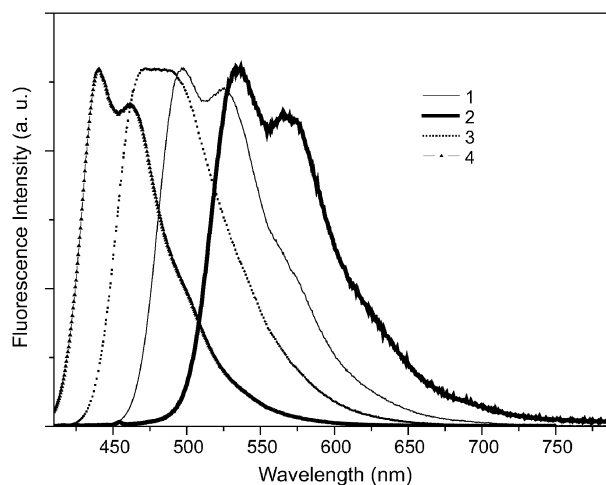


Fig. 5 Normalized, corrected fluorescence emission spectra of compounds **1–4** in THF (conc. $< 3 \times 10^{-6}$ M, 20 °C, $\lambda_{\text{exc}} = 400$ nm).

Photophysical properties of the zinc(II) complexes

Electronic absorption. Addition of an excess of ZnCl_2 or $\text{Zn}(\text{BF}_4)_2$ to solutions of ligands **1–3** induced a red-shift of the lowest energy transition band in the UV-visible spectrum ($\Delta\lambda$ *ca.* +3 to +28 nm), the value of the bathochromic shift being independent of the solvent nature (Table 2). The largest effect is recorded, as in the case of OPE-bridged ligands,²⁴ for the phenyl-terminated ligand **3**. So, even if the terminal bipyridine becomes more electron affinic upon zinc(II) complexation, the ground state does not present a significant charge transfer character. The modification of absorption spectrum of **1** in THF upon gradual addition of $\text{Zn}(\text{BF}_4)_2$ was used to monitor the metal complexation equilibrium which indicated the formation of a 1 : 1 (metal–ligand) complex with a stability constant $\log K$ of 5.5 ± 0.2 . The same value was found with the analogous OPE-bridged ligand²² and is of the same order of magnitude as that found for a related terpyridine complex.³⁷ The 1 : 1 stoichiometry was also confirmed by the synthesis and elementary analysis of the mononuclear zinc complex of **1** (see Synthesis).

Fluorescence emission. The most apparent ionochromic effects of ligands **1–3** upon complexation of zinc(II) are their instant colour changes from fluorescent blue (**3**), green (**1**) or yellow (**2**) to light orange (**3–ZnCl}_2**), orange (**1–ZnCl}_2**) or red (**2–ZnCl}_2**) in THF solution. Indeed, a considerable

Table 1 Photophysical properties of compounds **1–4**

| | Absorption | | Emission | | | | | | | |
|----------|---|---|----------------------------------|------------------------------|------------|----------------------------------|------------------------------|------------|------------------|---|
| | Toluene | THF | Toluene | | THF | | | | | |
| | $\lambda_{\text{max}}/\text{nm}$ ($\epsilon_{\text{max}}/\text{M}^{-1}\text{cm}^{-1}$) | $\lambda_{\text{max}}/\text{nm}$ ($\epsilon_{\text{max}}/\text{M}^{-1}\text{cm}^{-1}$) | $\lambda_{\text{max}}/\text{nm}$ | $\Delta\nu^a/\text{cm}^{-1}$ | Φ_f^b | $\lambda_{\text{max}}/\text{nm}$ | $\Delta\nu^a/\text{cm}^{-1}$ | Φ_f^b | τ/ns | $k_f/10^8 \text{ s}^{-1}$ ($k_f/n^3\nu^3/10^{-5} \text{ s}^{-1}\text{cm}^3$) |
| 1 | 430 (57 500) | 431 (45 600) | 493 | 2947 | 0.81 | 493 | 2910 | 0.82 | 1.69 | 4.9 (2.1) |
| 2 | 463 (99 900) | 463 (111 500) | 534 | 2889 | 0.70 | 534 | 2872 | 0.51 | 0.610 | 8.4 (4.6) |
| 3 | 404 (47 600) | 404 (62 130) | 462 | 3131 | 0.64 | 472 | 3566 | 0.64 | 1.61 | 4.0 (1.5) |
| 4 | 388 (27 140) | 388 (75 400) | 441 | 3123 | 0.79 | 440 | 3046 | 0.66 | ~1.6 | 4.1 (1.3) |

^a Stokes' shift. ^b Fluorescence quantum yield.

Table 2 Spectroscopic data for the zinc(II) complexes of compounds 1–3 in THF and in solvents of different polarity at room temperature^{a,b}

| | Absorption ^b | | Emission | | | | | | | | |
|---|----------------------------|---|----------------------------|-----|-----|------------|-----|-----|------------------------------------|---------------------|------------------------------|
| | λ_{\max}/nm | $\epsilon_{\max}/\text{M}^{-1}\text{cm}^{-1}$ | λ_{\max}/nm | | | | | | $\Delta\nu^{\circ}/\text{cm}^{-1}$ | $\rho^d/\text{\AA}$ | $\mu_{\text{ex}}^e/\text{D}$ |
| | | | TOL | EE | AE | THF | DCE | BN | | | |
| 1 | 455 (+25) | 43 600 | 558 | 591 | 605 | 611 (+118) | 628 | 638 | 5611 | 6.65 | 16 |
| 2 | 466 (+3) | 101 500 | 590 | ns | 643 | 655 (+121) | 670 | q | 6192 | 8.33 | 23 |
| 3 | 432 (+28) | 55 200 | 544 | 570 | 582 | 590 (+118) | 613 | 633 | 6199 | 6.25 | 15 |

^a q: quenched emission; ns: non-soluble. ^b For solvent abbreviations see experimental section. ^c Values in THF; in parentheses, bathochromic shifts relative to the free ligands. ^d Onsager cavity radius, approximated according to the solute density method, an average value of 1 g cm^{-3} being taken for the density. ^e Excited state dipole moment.

bathochromic shift of the fluorescence maximum ($\Delta\lambda$ ca. +120 nm) was obtained upon zinc(II) complexation (Table 2). The fluorescence emission spectra are not dependent on the excitation wavelength and the fluorescence excitation spectra were observed to match the absorption profiles. Furthermore, metal ion complexation is also accompanied by a broadening of the fluorescence emission bands along with a loss of vibronic structure. The half-height widths are observed to be larger than those of the free ligands (Fig. 6). These results, as well as the large Stokes' shifts, are consistent with fluorescence emission arising from a highly polar, charge transfer state. Moreover, this change in the nature of the excited state of the conjugated ligand upon zinc(II) chelation is intramolecular as the fluorescence emission spectrum of **4** is not affected upon addition of ZnCl_2 under the same conditions. Consistently, a strong solvatochromic effect is observed (Fig. 7 and Table 2), which is the result of the bipyridine ligand moiety becoming a strong withdrawing group upon zinc binding.²⁴ From the dependence of the emission maximum on the solvent polarity factor, an estimated value of the dipole moment of the excited state could be obtained for each ligand using the Lippert–Mataga equation (Table 2), assuming the ground state as weakly polar ($\mu_{\text{gs}} \approx 0$).³⁸ Indeed absorption maximum was found independent on solvent polarity. The high values obtained (μ_{ex} ca. +15 to +23 D) are in the range of those

calculated for OPE-bridged ligands and thus with the formation of a giant dipole along the molecular axis.³⁹ As in the case of the OPE-bridged ligands,²⁴ an increase of the dipole moment is observed with the increase in oligomer length. However, the dipole moment values calculated for the OPV ligands are found to be 20% lower than those calculated for the OPE corresponding ligands. This could be explained by a better efficiency in charge transfer of triple bonds compared to double bond, which is consistent with the results obtained by Ziesel and Harriman on acetylenic bridges.³⁵

Another effect of zinc(II) complexation is the decrease of fluorescence quantum yield as well as the increase fluorescence lifetimes, these observations being the most important in the case of the longest oligomer **2** (Table 3). All fluorescence decays recorded are still monoexponential in solvents such as toluene and THF. Given the very short temporal resolution (ca. 50 ps) of the time-resolved laser spectroscopy setup used in this study, this confirmed the occurrence of a single fluorescent complex species in solution in agreement with UV-visible titration results. The consequence of these results are a decrease of the radiative constants in the zinc(II) complex and a concomitant increase of the nonradiative rate, k_{nr} , in particular in the case of ligand **2**, as expected in the case of fluorescence emission from a low-lying charge transfer state (Table 3).

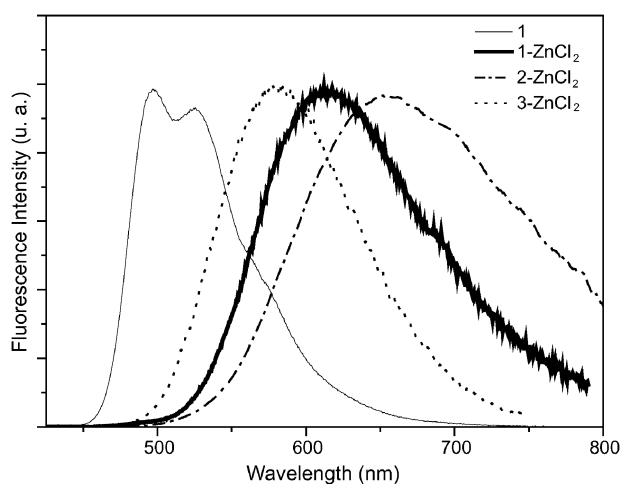


Fig. 6 Normalized, corrected fluorescence emission spectra of compounds 1–3 in the presence of an excess of ZnCl_2 in THF (ligand conc. $< 3 \times 10^{-6}$ M, metal conc. ca. 10^{-4} M, 20 °C, $\lambda_{\text{exc}} = 400$ nm).

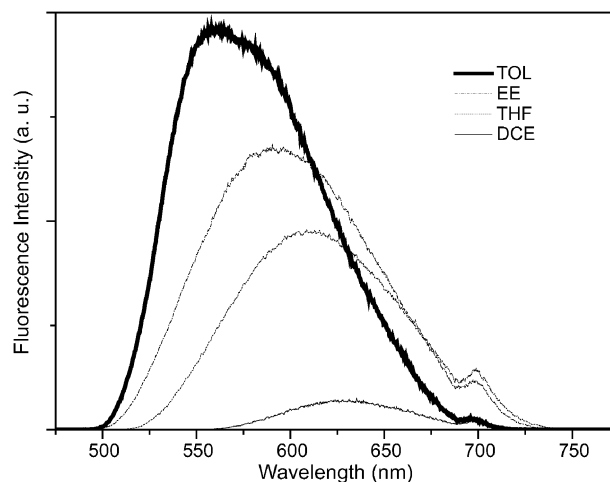


Fig. 7 Corrected fluorescence emission spectra of zinc(II) complexes of ligand **1** in solvents of increasing polarity (toluene, EE, THF, DCE). (ligand conc. $< 3 \times 10^{-6}$ M, metal conc. ca. 10^{-4} M, 20 °C, $\lambda_{\text{exc}} = 400$ nm).

Table 3 Photophysical properties of the zinc(II) complexes of compounds **1–3** in THF at room temperature

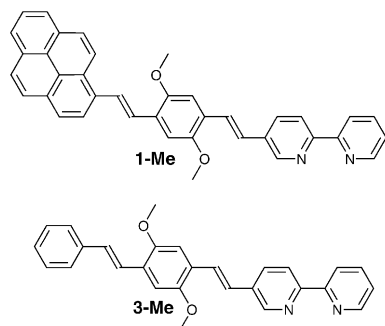
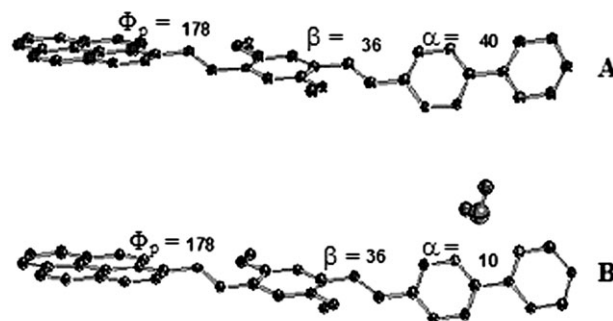
| | Φ_f | τ/ns | $k_f/10^8 \text{ s}^{-1}$ | $k_f n^{-3} \nu^{-3} / 10^{-5} \text{ s}^{-1} \text{ cm}^3$ | $k_{nr}/10^8 \text{ s}^{-1}$ |
|----------|----------|------------------|---------------------------|---|------------------------------|
| 1 | 0.28 | 2.05 | 1.4 | 1.1 | 3.51 |
| 2 | 0.04 | 0.317 | 1.3 | 1.3 | 30.3 |
| 3 | 0.43 | 2.80 | 1.5 | 1.1 | 2.04 |

Quantum chemical calculations

Quantum chemical calculations were performed in order to validate the spectroscopic results obtained in absence and presence of zinc(II) using the methylated model structures of **1–Me** and **3–Me** (Scheme 3), respectively.

The geometry of both models have been optimized at the Hartree–Fock semiempirical Austin model 1 (AM1) level. In the energetically most favourable ground-state structure found for free ligands, the non-substituted pyridine ring is twisted with respect to the other one by an angle α of 40° , consistent with literature data.^{24,31} In the case of ligand **1–Me**, the other important dihedral angle values are reported in Fig. 8A. The angle between pyrene and central benzene rings (Φ_p) is due to the steric interaction with the *peri* hydrogen and is consistent with the X-ray data (*vide supra*). Similarly, the value of the dihedral angle between the central aromatic ring and the first pyridine nucleus of the bipyridine unit (β) is found very close to that observed in the crystal. In the case of the corresponding zinc(II) complexes, the angle between the two pyridine rings was kept to zero and the results show no significant conformational reorganization of the conjugated backbone as compared to free ligand either for **1–Me** or **3–Me** (Fig. 8B for **1–Me**).

As was previously found for analogous acetylenic compounds,²⁴ the calculation show that the S_0 – S_1 transition is always the most important one both for free ligand and zinc(II) complexes, and involves molecular orbitals (MOs) that are of π character. However, in the case of free ligands, only one electronic transition (HOMO to LUMO) is necessary to describe the transition from the ground to the first excited state whereas for zinc(II) complexes, two electronic transitions (HOMO to LUMO and HOMO to LUMO + 1) are needed. Another interesting feature outlined by calculations, is the dependence of localization of the MOs on both the nature of the terminal aromatic nucleus and the presence of chelated zinc (II). Indeed, on one hand, in the case of free ligand **1–Me** both HOMO and LUMO are localized only on the pyrene and phenylene-vinylene bridge whereas in the case of **3–Me**, the

**Scheme 3** Structures of model ligands **1–Me** and **3–Me** as used in the semi empirical calculations.**Fig. 8** AM1 geometry optimisation of model ligand **1–Me** and its zinc(II) complex **1–Me–ZnCl₂**. The values of the dihedral angles Φ_p (between pyrene and central benzene rings), β (between the central aromatic ring and the first pyridine nucleus of the bipyridine unit) and α (between the two pyridine rings in the 2,2'-bipyridine) are given (see text).

HOMO orbital is localized from phenyl ring to the first pyridine ring of the bipyridine unit and the LUMO extends all over the molecular skeleton. This result confirmed the occurrence of a more polar excited state in the case of **3** than in the case of **1**, as outlined by the solvatochromic effect observed in the fluorescence study of **3**. On the other hand, upon chelation of zinc(II), an important effect on the localization of MOs was noticed. Indeed, the electronic density upon light excitation was shifted from the terminal aromatic nucleus and the phenylene-vinylene bridge for both **1–Me** and **3–Me** to the entire molecule in the case of **1–Me**, and to the phenylene-vinylene bridge and the bipyridine in the case of **3–Me**. The calculations thus confirm the increase of charge transfer character of the first excited state upon metal chelation.

Conclusion

As observed in the case of OPE-based ligands, the OPV counterparts described in this study are shown to exhibit strong emission colour modulation effect when they are exposed to zinc(II) ion. The emission colours were found to depend on the number of phenylene vinylene units in the conjugated backbone. As such they behave as an efficient class of Zn^{2+} -fluorogenic chemosensors or as tunable fluorophores for optoelectronic applications.

Experimental

General

Anhydrous zinc(II) chloride (Aldrich Chemical Co., 99.999%) was handled under an inert atmosphere using a glove box. All solvents used for spectroscopic measurements were of spectroscopic grade and were used as commercially available. The following are the abbreviations used for the solvents: toluene (TOL), diethyl ether (EE), ethyl acetate (AE), tetrahydrofuran (THF), dichloroethane (DCE), butyronitrile (BN), acetonitrile (AN). Electronic absorption spectra were recorded with a Hitachi U3300 spectrophotometer. Fluorescence spectra were recorded in non deoxygenated solvents at 20°C with either a Hitachi F4500 or a Spex Fluorolog spectrofluorimeter. We did

not find any difference in emission properties with and without degassing the solutions. Fluorescence quantum yields were determined using quinine sulfate as a standard ($\Phi_f = 0.55$ at 25 °C in 1 N H₂SO₄). The relative error in the quantum yields is $\pm 5\%$. Low-temperature experiments were carried out using a variable-temperature liquid nitrogen Optistat cryostat from Oxford instruments. The laser setup used in these experiments was as described elsewhere.²⁴

Syntheses

All chemicals were purchased from Aldrich Chemical Co. and were used as received. Solvents were distilled prior to use. ¹H and ¹³C NMR spectra were recorded with either a Bruker AC200 or a Bruker AC250 spectrometer. Mass spectra were obtained using a VG Autospec-Q Micromass spectrometer either in the EI or LSIM⁺ (NBA matrix) mode.

Pyrene-containing mono-aldehyde 5. To a solution of dialdehyde **6** (0.6 g, 0.54 mmol) and the pyrene-containing phosphonium salt (0.308 g, 0.54 mmol) in freshly distilled dichloromethane (100 mL) was added dropwise a solution of sodium ethanolate (0.6 mL, 1 M in ethanol) under an argon atmosphere at room temperature. The reaction mixture was stirred at room temperature for 4 h. The organic layer was then washed with water and dried over Na₂SO₄. The solvent was removed under vacuum and the crude product was subjected to column chromatography (silica gel) eluting with petroleum ether–dichloromethane (50 : 50 v/v). Compound **5**, an orange solid, was obtained as a mixture of *cis* and *trans* isomers which was used without further purification (0.36 g, 52% yield). ¹H NMR (200 MHz, CDCl₃), $\delta = 0.80$ – 0.91 (m, 18H, CH₃), 1.20–1.60 (m, 60H, CH₂), 1.80–2.00 (m, 12H, OCH₂CH₂), 3.98–4.12 (m, 12H, OCH₂), 7.00–8.36 (m, 15H, H_{aryl} and ethylene hydrogens), 10.43 (s, 0.55H, CHO), 10.45 (s, 0.45H, CHO).

Ligand 1. To a suspension of **7** (4.2 g, 4 mmol) in freshly distilled THF (60 mL), 95% NaH (0.65 g, 25.7 mmol) was added portionwise at room temperature. After dropwise addition of a solution of pyrene-1-carbaldehyde (0.92 g, 4 mmol) in THF (10 mL), the reaction mixture was heated at 30 °C and then a solution of 2,2'-bipyridine-5-carbaldehyde (0.8 g, 4.35 mmol) in THF (10 mL) was added dropwise. The reaction mixture was heated at 30 °C for 40 h, cooled down to room temperature and concentrated under vacuum. The crude product obtained was dissolved in dichloromethane. The organic layer was washed with water and dried over Na₂SO₄. The solvent was removed under vacuum and the crude product was subjected to column chromatography (silica gel) eluting with dichloromethane. The mixture of *cis* and *trans* isomers thus obtained was stirred with iodine (1.045 g, 4.11 mmol) in dichloromethane (125 mL) overnight at room temperature. The iodine was then quenched with a 1 M aqueous solution of Na₂S₂O₃. The organic layer was washed with brine, dried over Na₂SO₄ and concentrated under vacuum. The crude product was subjected to column chromatography (silica gel) eluting with dichloromethane and then crystallized from a mixture of dichloromethane–methanol. Compound **1** was obtained as the *trans* isomer (0.592 g, 20% yield) as an

orange solid. ¹H NMR (250 MHz, CDCl₃), $\delta = 0.81$ – 0.91 (m, 6H, CH₃), 1.20–1.66 (m, 20H, CH₂), 1.87 (m, 4H, OCH₂CH₂), 4.12–4.19 (m, 4H, OCH₂), 7.21 (s, 1H, H_{phenyl}), 7.22 (d, 1H, $J = 16.5$ Hz, CH=CH), 7.31 (s, 1H, H_{phenyl}), 7.31–7.38 (m, 1H, H₅), 7.66 (d, 1H, $J = 16.5$ Hz, CH=CH), 7.69 (d, 1H, $J = 16.2$ Hz, CH=CH), 7.87 (td, 1H, $J_1 = 9.85$ Hz, $J_2 = 2.15$ Hz, H₄), 8.00–8.38 (m, 10H, CH=CH, H₄ and H_{pyr}), 8.45–8.49 (m, 2H, H₃ and H_{3'}), 8.53 (d, 1H, $J = 9.5$ Hz, H_{2pyr}), 8.71–8.73 (m, 1H, H₆), 8.83 (s, 1H, H₆). MS (EI), m/z : 740 (M⁺). Analysis calc. (found) for C₅₂H₅₆N₂O₂: C, 84.28(83.88); H, 7.62(7.23); N, 3.78(3.93)%.

Ligand 2. To a solution of **5** (0.31 g, 0.22 mmol) and the phosphonium salt of 5-bromomethyl-2,2'-bipyridine (0.169 g, 0.33 mmol) in freshly distilled dichloromethane (75 mL) was added dropwise a solution of lithium ethanolate (0.37 mL, 1 M in ethanol) under argon atmosphere at room temperature. The reaction mixture was stirred at room temperature for 4 h. The organic layer was then washed with water and dried over Na₂SO₄. The solvent was removed under vacuum and the crude product was subjected to column chromatography (silica gel) eluting with dichloromethane–methanol (99 : 1 v/v). The mixture of *cis* and *trans* isomers thus obtained was stirred with iodine (0.5 g, 1.96 mmol) in dichloromethane (60 mL) for 24 h at room temperature. The iodine was then quenched with a 1 M aqueous solution of Na₂S₂O₃. The organic layer was washed with brine, dried over Na₂SO₄ and concentrated under vacuum. The crude product was subjected twice to column chromatography (silica gel) eluting with dichloromethane and then crystallized from a mixture of dichloromethane–methanol. Compound **2** was obtained as the *trans* isomer (0.16 g, 50% yield) as an orange solid. ¹H NMR (200 MHz, CD₂Cl₂), $\delta = 0.84$ – 0.93 (m, 18H, CH₃), 1.30–1.62 (m, 60H, CH₂), 1.84–1.99 (m, 12H, OCH₂CH₂), 4.00–4.19 (m, 12H, OCH₂), 7.21–7.35 (m, 8H, CH=CH and H_{phenyl}), 7.24 (d, 1H, $J = 17.2$ Hz, CH=CH), 7.31 (m, 1H, H₅), 7.55 (s, 1H, H_{phenyl}), 7.58 (s, 1H, H_{phenyl}), 7.66 (d, 1H, $J = 17.2$ Hz, CH=CH), 7.77 (d, 1H, $J = 16.5$ Hz, CH=CH), 7.83 (td, 1H, $J = 7.6$ Hz, H₄), 8.37 (d, 1H, $J = 16.5$ Hz, CH=CH), 7.98–8.46 (m, 11H, H₃, H_{3'}, H₄ and H_{pyr}), 8.53 (d, 1H, $J = 9.4$ Hz, H_{2pyr}), 8.65–8.68 (m, 1H, H₆), 8.79 (s, 1H, H₆). MS (LSIMS⁺), m/z : 1458 (M + 1). Analysis calc. (found) for C₁₀₀H₁₃₂N₂O₆: C, 82.41(81.34); H, 9.06(9.30); N, 1.92(1.98)%.

Ligand 3. To a solution of **7** (3.69 g, 3.5 mmol), 2,2'-bipyridine-5-carbaldehyde (0.65 g, 3.5 mmol) and benzaldehyde (0.36 mL, 3.54 mmol) in freshly distilled dichloromethane (150 mL) was added dropwise a solution of lithium ethanolate (9.1 mL, 1 M in ethanol) under argon atmosphere at room temperature. The reaction mixture was stirred at room temperature for 0.5 h and then poured onto a diluted aqueous chlorhydric acid solution. The organic layer was then washed with water and dried over Na₂SO₄. The solvent was removed under vacuum. The mixture of *cis* and *trans* isomers thus obtained was stirred with iodine (1.7 g, 6.7 mmol) in dichloromethane (150 mL) overnight at room temperature. The iodine was then quenched with a 1 M aqueous solution of Na₂S₂O₃. The organic layer was washed with water, dried over

Na₂SO₄ and concentrated under vacuum. The crude product was subjected twice to column chromatography: first on deactivated alumina with petroleum ether–dichloromethane (5 to 100%) mixture as eluant and second on silica gel with dichloromethane–methanol (1 to 4%) mixture as eluant. Compound **3** was obtained as the *trans* isomer (0.238 g, 11% yield) as an orange solid. ¹H NMR (250 MHz, CDCl₃), δ = 0.83–0.92 (m, 6H, CH₃), 1.20–1.60 (m, 20H, CH₂), 1.88 (m, 4H, OCH₂CH₂), 4.07 (t, 2H, *J* = 6.4 Hz, OCH₂), 4.08 (t, 2H, *J* = 6.4 Hz, OCH₂), 7.16 (d, 1H, *J* = 16.5 Hz, CH=CH), 7.14–7.56 (m, 9H, CH=CH, H_{5'}, and H_{phenyl}), 7.43 (d, 1H, *J* = 16.5 Hz, CH=CH), 7.61 (d, 1H, *J* = 16.5 Hz, CH=CH), 7.83 (td, 1H, *J*₁ = 7.6 Hz, *J*₂ = 1.8 Hz, H_{4'}), 7.99 (dd, 1H, *J*₁ = 8.2 Hz, *J*₂ = 2.1 Hz, H₄), 8.38–8.42 (m, 2H, H₃ and H_{3'}), 8.69 (d, 1H, *J* = 4.6 Hz, H_{6'}), 8.79 (d, 1H, *J* = 2.1 Hz, H₆). MS (EI), *m/z*: 616 (M⁺). Analysis calc. (found) for C₄₂H₅₂N₂O₂: C, 81.78(81.68); H, 8.50(8.69); N, 4.54(4.46).

1,4-Bis(octyloxy)-2,5-distyrylbenzene 4. To a solution of **7** (1.85 g, 1.77 mmol), and benzaldehyde (0.36 mL, 3.54 mmol) in freshly distilled dichloromethane (75 mL) was added dropwise a solution of lithium ethanolate (5 mL, 1 M in ethanol) under argon atmosphere at room temperature. The reaction mixture was stirred at room temperature overnight and then poured onto a diluted aqueous chlorhydric acid solution. The organic layer was then washed with water and dried over Na₂SO₄. The solvent was removed under vacuum. The mixture of *cis* and *trans* isomers thus obtained was stirred with iodine (0.9 g, 3.54 mmol) in dichloromethane (80 mL) for 24 h at room temperature. The iodine was then quenched with a 1 M aqueous solution of Na₂S₂O₃. The organic layer was washed with water, dried over Na₂SO₄ and concentrated under vacuum. The crude product was subjected twice to column chromatography: first on silica gel with petroleum ether–dichloromethane (75 : 25 v/v) mixture as eluant and second on deactivated alumina with petroleum ether–dichloromethane (0 to 25%) mixture as eluant. Compound **4** was obtained as the *trans* isomer (0.52 g, 55% yield) as a yellow solid. ¹H NMR (200 MHz, CDCl₃), δ = 0.83–0.92 (m, 6H, CH₃), 1.20–1.56 (m, 20H, CH₂), 1.88 (q, 4H, *J* = 7.9 Hz, OCH₂CH₂), 4.06 (t, 4H, *J* = 6.4 Hz, OCH₂), 7.10–7.56 (m, 12H, H_{phenyl} and CH=CH), 7.13 (s, 2H, H_{phenyl}), 7.14 (d, 2H, *J* = 16.5 Hz, CH=CH). MS (EI), *m/z*: 538 (M⁺). Analysis calc. (found) for C₃₈H₅₀O₂: C, 84.76(83.92); H, 9.29(9.29)%.

Mononuclear zinc(II) complex of ligand 1 (1–ZnCl₂). A suspension of **1** (30 mg, 0.04 mmol) and ZnCl₂ (6.8 mg, 0.05 mmol) in freshly distilled dichloromethane (10 mL) was stirred for 24 h in darkness at room temperature. The solvent was then removed under vacuum. The solid thus obtained was washed with diethyl ether and dried under vacuum to afford **1–Zn** as a red powder (24.6 mg, 65% yield). Analysis calc. (found) for C₅₂H₅₆N₂O₂ZnCl₂: C, 71.03(69.69); H, 6.65(6.31); N, 3.19(3.23); Cl, 8.06(8.09); Zn, 7.43(6.84)%.

Quantum chemical calculations

The input geometries were optimized by a semi-empirical restricted Hartree–Fock method using the AM1 Hamiltonian within the AMPAC program.⁴⁰ The influence of the different

twist angles between two adjacent rings was systematically investigated. To be sure that the optimized geometry corresponds to the lowest energy, vibrational frequencies were also determined.⁴¹ Excited state energies were obtained for each optimized ground-state geometry by single configuration interaction method involving excitations from 10 occupied to 10 unoccupied molecular orbitals. As the number of possible excitations was huge, a truncation of the configuration interaction active space was made, as the lowest-energy excited states are of main interest. Care was taken to ensure that the energies and oscillator strengths of the transitions of interest were not significantly dependent on the number of configurations used in the calculation.

X-ray crystallography

Data were collected at 293 K on a STOE-IPDS diffractometer equipped with a graphite monochromator utilizing Mo Kα radiation (λ = 0.71073 Å). The structure was solved and refined on *F*² by full matrix least-squares techniques using SHELX-97 package. All non-H atoms were refined anisotropically and the H atoms were included in the calculation without refinement. Absorption was corrected by gaussian technique.

Crystal data† for **1**: C₅₂H₅₆N₂O₂, *M* = 740.99, triclinic, space group *P*1̄, *a* = 9.0140(8) Å, *b* = 14.873(2) Å, *c* = 16.749(2) Å, α = 77.96(1)°, β = 83.05(1)°, γ = 77.57(1)°, *V* = 2137.8(4) Å³, *Z* = 2, ρ_{calc} = 1.151 g cm⁻³, μ(Mo Kα) = 0.069 mm⁻¹, *F*(000) = 796, θ_{min} = 2.07°, θ_{max} = 25.98°, 20 865 reflections collected, 7724 unique (*R*_{int} = 0.0545), restraints/parameters = 0/507, *R*1 = 0.0471 and *wR*2 = 0.1123 using 3089 reflections with *I* > 2σ(*I*), *R*1 = 0.1248 and *wR*2 = 0.1413 using all data, GOF = 0.794, -0.135 < Δρ < 0.339 e Å⁻³.

References

- P. F. H. Schwab, M. D. Levin and J. Michl, *Chem. Rev.*, 1999, **99**, 1863.
- P. F. H. Schwab, J. R. Smith and J. Michl, *Chem. Rev.*, 2005, **105**, 1197.
- T. Goodson III, W. Li, A. Ghadavi and L. Yu, *Adv. Mater.*, 1997, **9**, 639.
- T. C. Gorjanc, I. Lévesque and M. D'Ororio, *Appl. Phys. Lett.*, 2004, **84**, 930.
- J.-F. Eckert, J.-F. Nicoud, J.-F. Nierengarten, S.-G. Liu, L. Echegoyen, N. Armaroli, F. Barigelletti, L. Ouali, V. Krasnikov and G. Hadziioannou, *J. Am. Chem. Soc.*, 2000, **122**, 7467.
- E. E. Neuteboom, S. C. J. Meskers, P. A. van Hal, J. K. J. van Duren, E. W. Meijer, R. A. J. Janssen, H. Dupin, G. Pourtois, J. Cornil, J.-L. Brédas and D. Beljonne, *J. Am. Chem. Soc.*, 2003, **125**, 8625.
- W. Zhu, W. Li and L. Yu, *Macromolecules*, 1997, **30**, 6274–6279.
- A. P. H. J. Schenning, E. Peeters and E. W. Meijer, *J. Am. Chem. Soc.*, 2000, **122**, 4489.
- C. R. L. P. N. Jeukens, P. Jonkheijm, F. J. P. Wijnen, J. C. Gielen, P. C. M. Christianen, A. P. H. J. Schenning, E. W. Meijer and J. C. Mann, *J. Am. Chem. Soc.*, 2005, **127**, 8280.
- A. Ajayaghosh and S. J. George, *J. Am. Chem. Soc.*, 2001, **123**, 5148.
- K. Tajima, L.-S. Li and S. I. Stupp, *J. Am. Chem. Soc.*, 2006, **128**, 5488.
- P. F. Van Hutten, V. V. Krasnikov and G. Hadziioannou, *Acc. Chem. Res.*, 1999, **32**, 257.
- D. Oelkrug, A. Tompert, J. Gierschner, H.-J. Egelhaaf, M. Hanack, M. Hohloch and E. Steinhuber, *J. Phys. Chem. B*, 1998, **102**, 1902.

- 14 N. Armaroli, J.-F. Eckert and J.-F. Nierengarten, *Chem. Commun.*, 2000, 2105.
- 15 S. J. George and A. Ajayaghosh, *Chem.–Eur. J.*, 2005, **11**, 3217.
- 16 X.-y. Wang, A. Del Guerso and R. H. Schmehl, *Chem. Commun.*, 2002, 2344.
- 17 J.-M. Rueff, J.-F. Nierengarten, P. Gilliot, A. Demessence, O. Cregut, M. Drillon and P. Rabu, *Chem. Mater.*, 2004, **16**, 2933.
- 18 S. Leroy-Lhez and F. Fages, *C. R. Chim.*, 2005, **8**, 1204–1212.
- 19 B. Wang and M. R. Wasielewski, *J. Am. Chem. Soc.*, 1997, **119**, 12.
- 20 L. X. Chen, W. J. H. Jäger, D. J. Gosztola, M. P. Niemczyk and M. R. Wasielewski, *J. Phys. Chem. B*, 2000, **104**, 1950.
- 21 R. C. Smith, A. G. Tennyson, M. H. Lee and S. J. Lippard, *Org. Lett.*, 2005, **7**, 3573.
- 22 S. Leroy, T. Soujanya and F. Fages, *Tetrahedron Lett.*, 2001, **42**, 1665.
- 23 S. Leroy-Lhez and F. Fages, *Eur. J. Org. Chem.*, 2005, 2684.
- 24 S. Leroy-Lhez, A. Parker, P. Lapouyade, C. Belin, L. Ducasse, J. Oberlé and F. Fages, *Photochem. Photobiol. Sci.*, 2004, **3**, 949.
- 25 S. Leroy-Lhez, C. Belin, A. D'Aléo, R. M. Williams, L. De Cola and F. Fages, *Supramol. Chem.*, 2003, **15**, 627.
- 26 J. Polin, E. Schmohel and V. Balzani, *Synthesis*, 1998, 321.
- 27 A. Hilton, T. Renouard, O. Maury, H. Le Bozec, I. Ledoux and J. Zyss, *Chem. Commun.*, 1999, 2521.
- 28 A. L. Rodriguez, G. Peron, C. Duprat, M. Vallier, E. Fouquet and F. Fages, *Tetrahedron Lett.*, 1998, **39**, 1179.
- 29 H. Li, D. R. Powell, R. K. Hayashi and R. West, *Macromolecules*, 1998, **31**, 52.
- 30 T. Soujanya, A. Philippon, S. Leroy, M. Vallier and F. Fages, *J. Phys. Chem. A*, 2000, **104**, 9408.
- 31 H. Meier, J. Gerold, H. Kolshorn and B. Mühlring, *Chem.–Eur. J.*, 2004, **10**, 360.
- 32 H. Meier, *Angew. Chem., Int. Ed.*, 2005, **44**, 2482.
- 33 L. Viau, O. Maury and H. Le Bozec, *Tetrahedron Lett.*, 2004, **45**, 125.
- 34 J. K. Kochi and G. S. Hammond, *J. Am. Chem. Soc.*, 1953, **75**, 3452.
- 35 A. C. Benniston, A. Harriman, V. Grosshenny and R. Ziessel, *New J. Chem.*, 1997, **21**, 405.
- 36 K. A. Walters, K. D. Ley and K. S. Schanze, *Chem. Commun.*, 1998, 1115.
- 37 A. C. Benniston, A. Harriman, D. J. Lawrie, A. Mayeux, K. Rafferty and O. D. Russell, *Dalton Trans.*, 2003, 4762.
- 38 M. Maus, W. Rettig, D. Bonafoux and R. Lapouyade, *J. Phys. Chem. A*, 1999, **103**, 3388.
- 39 H. Le Bozec and T. Renouard, *Eur. J. Inorg. Chem.*, 2000, 229.
- 40 (a) AMPAC 6.0: Semichem, 7204 Mullen, Shawnee, KS 66216, USA, 1997; (b) M. J. S. Dewar, E. G. Zebisch, E. F. Healy and J. P. Stewart, *J. Am. Chem. Soc.*, 1985, **107**, 3902.
- 41 D. C. Young, *Computational Chemistry*, Wiley-Interscience, Weinheim, 2001, chap. 11.